

## Effect of pH values on the structural, morphological and sensing properties of ZnO nanostructure

A. Zaidi<sup>a</sup>, K. Tiwari<sup>a</sup>, R.R. Awasthi<sup>b</sup>, K.C. Dubey<sup>c,\*</sup>

<sup>a</sup>Department of Physics, B.B.D. University, Lucknow-226020, U.P., India

<sup>b</sup>Faculty of engineering and technology, Khwaja Moinuddin Chisti Language University, Lucknow- 226013, U.P., India

<sup>c</sup>Department of Physics, Shia P.G. College, Lucknow-226003, U.P., India

In the present investigation ZnO thin films have been prepared by sol-gel spin coating technique with different pH values. The effect of pH values of precursor solution on the crystal structural, morphological and humidity sensing properties of ZnO nanostructures have been investigated using different characterization technique. The crystal structure and phase analysis has been examined by powder X-ray diffraction (PXRD) technique. The PXRD pattern clearly revealed the ZnO thin films have hexagonal wurtzite crystal structure. The average crystallite size of ZnO thin films have been calculated using Scherer formula and found to be ~24 nm to ~30 nm. The microstrain ( $\epsilon_a$ ) and ( $\epsilon_c$ ) of ZnO thin films for different pH values 8 and 11, have been calculated and found to be 7.59, 0.1017; 7.57, 0.1094 respectively. The scanning electron microscopy (SEM) image depicts the formation of spherical nanostructure with diameter range 80 to 95 nm distributed throughout the surface. The atomic force microscopy (AFM) image also shows the spherical nanostructure consistently distributed throughout the surface with diameter range 75 to 80 nm. It was also found that increasing the pH values from 8 to 11 modified the grains and grains boundary. The humidity sensing properties of ZnO thin films prepared from pH values of 8 to 11 and found to be lower hysteresis loss, less aging effect and good sensitivity in the range of 8.37 M $\Omega$ /%RH to 12.25 M $\Omega$ /%RH respectively.

(Received October 3, 2022; Accepted January 6, 2023)

*Keywords:* ZnO, pH, Humidity, XRD, SEM, AFM

### 1. Introduction

Metal oxides semiconducting nanostructures such as zinc oxide (ZnO), tin oxide (TiO<sub>2</sub>), tin oxide (SnO<sub>2</sub>) etc. have been extensively investigated in current years due to its prospective applications in functional device [1-6]. Among these metal oxides, ZnO nanomaterials have gained more importance compared to others because of its non-toxicity and low inexpensive. ZnO nanostructures is a wide optical band gap (3.37 eV) semiconducting nanomaterials with a large exciton binding energy of 60 meV at room temperature with unique chemical, optical, physical, dielectric and sensing properties. ZnO semiconducting nanomaterial has attracted great attention due to its considerable significance of various novel functional applications such as humidity and gas sensor, optoelectronics devices, solar cells and several other essential modern applications. There are various methodologies have been reported by several research groups for deposition of ZnO nanostructures. The researchers have used various other synthesis techniques, for preparation of ZnO nanomaterials such as wet chemical techniques, physical vapor deposition, metal organic chemical vapor deposition, hydrothermal, pulsed laser deposition, molecular beam epitaxy (MBE), sputtering, electro spinning etc. [9-22]. The preponderance of these synthesis techniques is performed at high temperature and requires very expensive instrumentation. Furthermore synthetic fabrication of metal oxide nanomaterials is very dangerous for human being due to its environmental pollution. To suppress the above problem, the sol-gel spin coating chemical approach is comparatively very simple, less expensive and easy to doping and reliable method a

---

\*Corresponding author: krishnacubey@gmail.com  
<https://doi.org/10.15251/CL.2023.201.33>

non-toxic, easy to doping, inexpensive, and environmental eco-friendly sol-gel spin coating technique using ethylene glycol as stabilizing and reducing agent. In the present research paper we have studied the effect of pH values on the structural, morphological and dielectric properties of ZnO nanostructure synthesized by sol-gel spin coating method.

## 2. Experimental section

In the present research work, ZnO nanostructure thin films have been synthesized by sol-gel spin coating technique. The zinc acetate [ $\text{Zn}(\text{CH}_3\text{COO})_2 \cdot 2\text{H}_2\text{O}$ ] have been dissolve in concentrated nitric acid and adding 1N sodium hydroxide for basic bath. The resultant precursor solutions were continuously stirred for 6 hours on a magnetic stirrer. As a result the homogeneous and transparent precursor solution was obtained. The pH values of precursor solutions were adjusted by adding different quantities of 1N sodium hydroxide (NaOH) in the transparent aqueous solution. The transparent precursor solutions have been prepared with different pH values varied from 8 and 11. These homogeneous transparent precursor solutions were stirred using magnetic starrer for 8 h at room temperature. The prepared precursor solution with different pH values 8 and 11 was used for preparations of ZnO nanostructure thin films. The synthesized thin films were annelid at  $450^\circ\text{C}$  for 2 h in an open atmosphere. The synthesize ZnO thin films have been characterized by X-ray diffraction (XRD), using Rigaku Ultima IV,  $\text{CuK}\alpha$  ( $\sim 1.5406 \text{ \AA}$ ) radiation, scanning electron microscopy (SEM) and Agilent network with impedance analyzer with LCR meter.

## 3. Results and discussion

### 3.1. X-ray diffraction analysis

The powder X-ray diffraction (XRD) patterns of ZnO thin films synthesized with different pH values 8 and 11 are shown in figure 1.

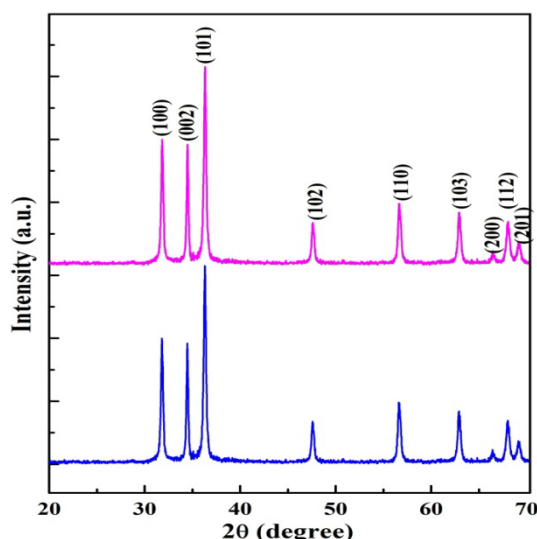


Fig. 1. XRD patterns of ZnO thin films for pH 8 and 11 precursor solution.

The X-ray diffraction pattern of ZnO thin films well matches with the (JCPDS card No 75-0576) and clearly shows that hexagonal wurtzite crystal structure with  $P6_3mc$  space group. However X-ray diffraction pattern of ZnO thin films shows no other reflection of impurities peaks indicating that sample is highly pure. The presence of broad diffraction peaks in X-ray diffraction

patterns such as (100), (002), (101), (102), (110), (103), (200), (112), (201) plane present in sample shows the polycrystalline hexagonal wurtzite structure of ZnO with P63mc space group. The average crystallite size ( $D$ ) of the ZnO thin films samples have been calculated by Scherrer formula [20]:

$$D = \frac{K \lambda}{\beta \cos \theta} \quad (1)$$

where  $K$  is constant ( $K=0.9$ ),  $\lambda$  is the X-ray wavelength used in XRD ( $\text{CuK}\alpha$ ),  $\theta$  is the Bragg angle,  $\beta$  is full-width at half-maximum (FWHM). The average crystallite size of ZnO thin film prepared with different pH concentration 8 and 11 was calculated from Scherrer formula and found to be  $\sim 24$  and  $\sim 30$  nm respectively.

The structural characteristics lattice-constants ( $a$  &  $c$ ) are also calculated from XRD data using peak-position ( $\theta$ ) and  $\lambda$  is X-ray diffraction wavelength  $1.5406 \text{ \AA}$ .

$$a = \sqrt{\frac{1}{3} \frac{\lambda}{\sin \theta}} \quad (2)$$

$$c = \frac{\lambda}{\sin \theta} \quad (3)$$

The lattice parameters of ZnO thin films unit cell have been calculated using equation 2 & 3 and found to be  $a = b = 3.0031 \text{ \AA}$ ,  $c = 5.2047 \text{ \AA}$ ;  $a = b = 3.0039 \text{ \AA}$ ,  $c = 5.2043 \text{ \AA}$  at different pH values 8 and 11 respectively. The micro-strains ( $\epsilon_a$ ) and ( $\epsilon_c$ ) of ZnO thin films for different pH values 8 and 11, have been calculated along a & c axis respectively.

$$\epsilon_a = \frac{a - a_0}{a_0} \times 100 \quad (4)$$

$$\epsilon_c = \frac{c - c_0}{c_0} \times 100 \quad (5)$$

where  $a_0$  and  $c_0$  are standard lattice constant without micro-strain to be;  $a_0 = 3.25 \text{ \AA}$  and  $c_0 = 5.21 \text{ \AA}$  used with JCPDS card No 75-0576. The micro-strain ( $\epsilon_a$ ) and ( $\epsilon_c$ ) of ZnO thin films for different pH values 8 and 11, have been calculated and found to be 7.59, 0.1017; 7.57, 0.1094 respectively. The values of micro-strain ( $\epsilon_a$ ) slightly decreases along a-axis from 7.59 to 7.57 and ( $\epsilon_c$ ) increases along c-axis from 0.1017 to 0.1094 may be due to lattice mismatch between ZnO thin films and glass substrate. The positive sign of micro-strains values signify that tensile-strain present in ZnO thin films due to expansion of the lattice constants.

$$\delta = \frac{1}{D^2} \quad (6)$$

The dislocation density (defects) present in ZnO thin films crystal is estimated by the equation 6. The bond length ( $L$ ) and volume ( $V$ ) of hexagonal crystal of ZnO nanostructures can be calculated by following equations,

$$L = \sqrt{\left[ \frac{a^2}{3} + \left( \frac{1}{2} - u \right)^2 c^2 \right]} \quad (7)$$

$$u = \left[ \frac{a^2}{3c^2} + 0.25 \right] \quad (8)$$

$$V = \left[ \left( \frac{\sqrt{3}}{2} \right) a^2 c \right] \quad (9)$$

where  $u$  is the positional parameter of hexagonal crystal of ZnO nanostructures associated with lattice constant ( $a/c$ ) ratio. The bond length of ZnO nanostructure have been calculated and found to be  $0.3609 \text{ \AA}$  and  $0.3611 \text{ \AA}$  for different pH values 8 and 11 respectively. It is also found that

bond length increases with increasing pH values may be due to modification of lattice constant constant ( $a/c$ ) ratio. Furthermore volume of hexagonal crystal of ZnO nanostructures have been also calculated and found to be 41.588 Å and 41.6070 Å for different pH values 8 and 11 respectively. The volume of hexagonal unit cell of ZnO thin films also slightly increases with increasing pH values it may be due to increasing the lattice constant.

### 3.2. Scanning electron microscopy analysis

The SEM micrographs of ZnO thin films for different pH values 8 and 11 have been observed at constant magnifications X3000 as shown in figure 2(a)-(b). The surface morphology reveals the formation of spherical shaped nanoparticles with granular structures for different pH values 8 and 11. The SEM image also clearly visualizes the asymmetrical spherical shape nanostructure uniformly distributed throughout the sample surface formation with high packing density. The SEM images of ZnO thin films for different pH values 8 and 11 shows diffused grains and grain boundary with particles size ranging between 80 and 95 nm. The particles sizes were seen to slightly increase with increasing pH concentrations. These SEM micrographs clearly revealed that the particles have very small agglomeration as a result they have asymmetrical and spherical irregular in shape. The observed asymmetrical and irregularity shape particles in SEM images indicates that synthesized nanoparticles containing large volume to surface ratio. Figure 2(c)-(d) shows the histogram of SEM image which exhibits that ZnO thin films for different pH values 8 and 11 have uniform particles size distribution. The software program Image J (version 1.46r) was used for SEM image analysis. The observed standard deviations and mean deviations of ZnO thin films for different pH values 8 and 11 using Image J software and found to be 34.479, 38.586 and 129.460, 136.359 respectively. Consequently, the standard deviation revealed that pixels spread out around the mean of the crystallite. The mean deviation is measured the closest alternative to standard deviation. Thus, the instability of the SEM micrograph is expressed as a significance of standard deviation. Figure 3(a-b) shows the hill stack surface plot of SEM image using the Image J software. Hill stack surface plot show that improved crystalline behavior of the ZnO thin films for increases the pH values of precursor solutions.

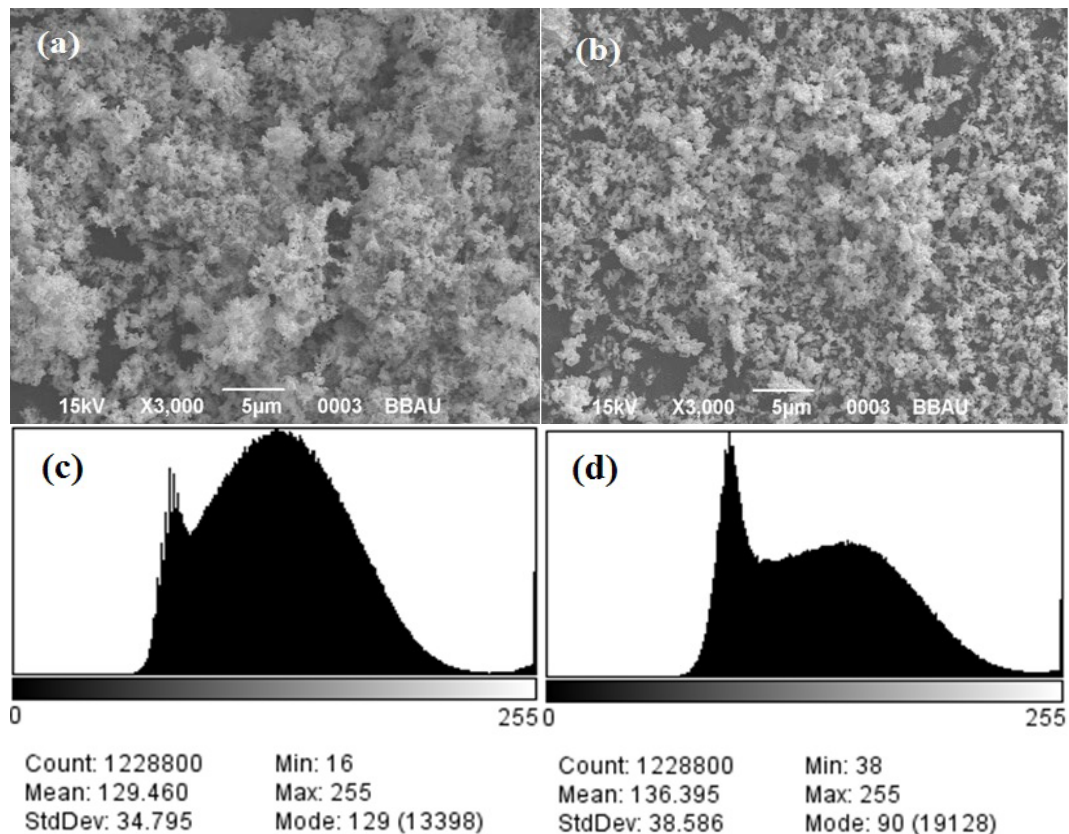


Fig. 2. SEM images of ZnO thin films for pH 8 and 11 precursor solution.

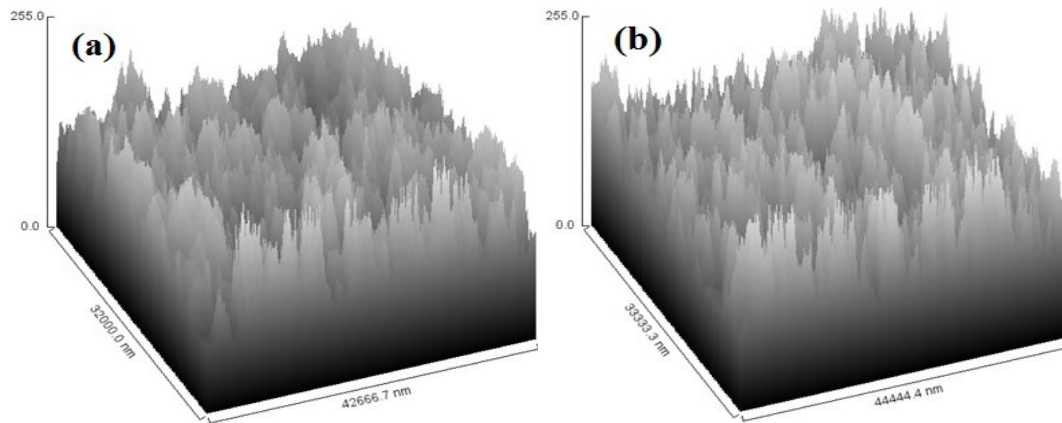


Fig. 3. Figure 3(a-b) shows the hill stack surface plot of SEM image.

### 3.3. Atomic force microscopy analysis

The figure 4(a)-(b) shows surface morphology of ZnO thin films prepared to different pH values 8 and 11 by sol gel spin coating technique.

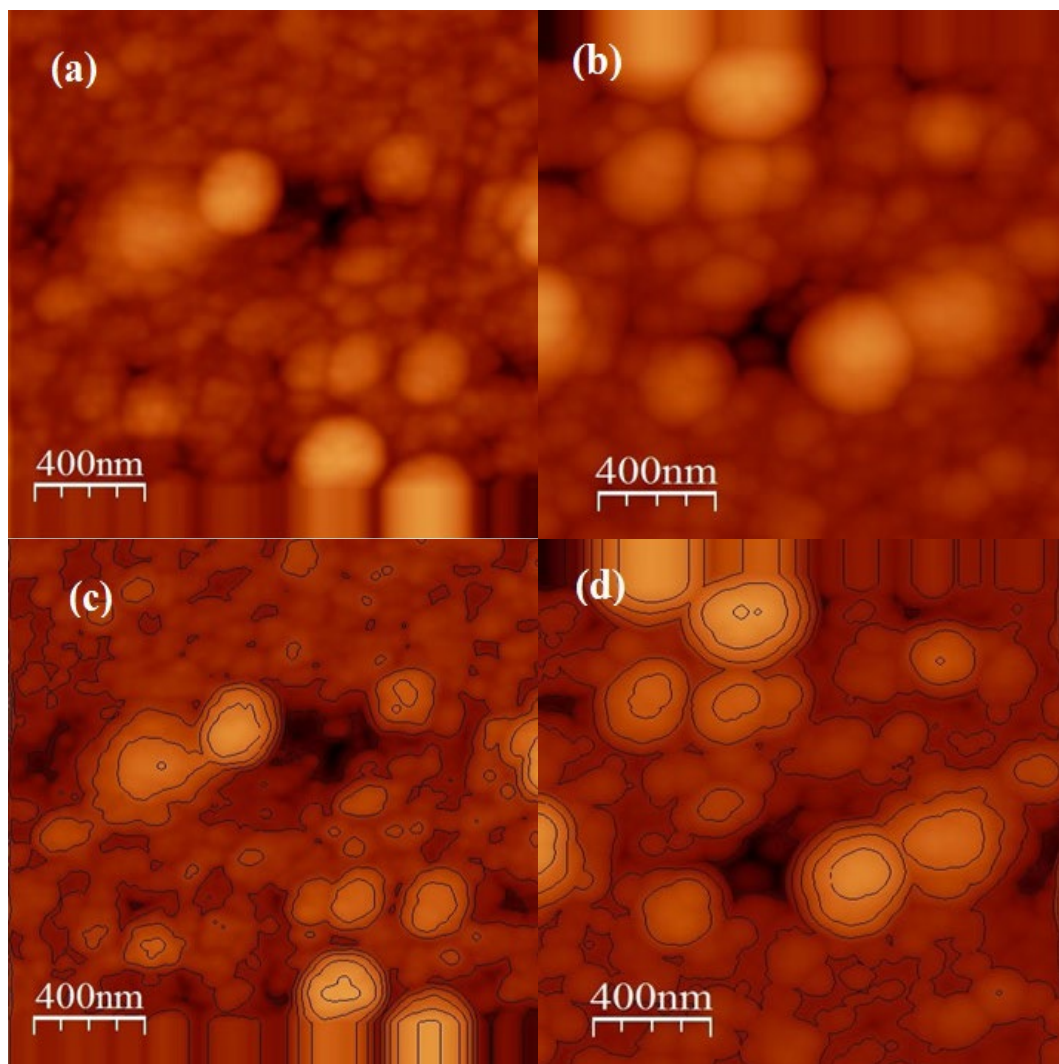


Fig. 4. (a-b) 2D, AFM images and (c-d) high resolution contour plot of ZnO thin films.



It micrograph reveals that the formation of spherical particles with granular growth of ZnO thin films sample. The particle sizes of ZnO thin films prepared to different pH values 8 and 11 have been observed from AFM image and found to be about ~75 nm and ~80 nm respectively. The particles sizes slightly increases with increasing pH values of precursor solution which is in venerable consistency with the powder X-ray diffraction result. The SEM measurements also revealed that particles size increases with increasing pH concentration of precursor solution. The surface parameters, such as root mean square (RMS) surface roughness of ZnO thin films prepared for different pH values 8 and 11 have been observed and found to be ~13.56 nm to 8.67 nm respectively. Thus decrease the surface roughness with increasing pH values indicating the enhancement of surfaces smoothness and uniformity of the sample. Figure 4(c)-(d) exhibited the high resolution contour plot of AFM images, which demonstrate that ZnO thin films prepared for different pH values 8 and 11 have asymmetric growth of grains in-plane shapes with spherical and elliptical bases. Furthermore ZnO thin films prepared for different pH values 11 contour plots clearly revealed that suppress the asymmetric growth and increase the in-plane symmetrical growth with spherical bases.

### 3.4. Humidity sensing and sensitivity analysis

The studies of humidity sensing properties of ZnO thin films have been prepared on glass substrate from different pH values 8 and 11. For humidity sensing applications ZnO thin films sample placed in a humidity control chamber in which purified of potassium sulphate ( $K_2SO_4$ ) has been used as a humidifier and potassium hydroxide (KOH) as a dehumidifier. The variation of resistance was recorded corresponding to the change in humidity level. The variation of resistance verses change in %RH have been recorded by using standard hygrometer for the sensing materials of different pH values 8 and 11 shown in figure 5. It is observed that resistance continuously decrease with increasing the %RH in the range of (<50%RH) which may be due to excellent conductivity of the ZnO thin films sample. The humidity gas sensing measurement results revealed that ZnO thin films prepared from different pH values 8 and 11 displayed fast response characteristics as well as good reproducibility. Sensitivity =  $\Delta R/\Delta \%RH$  of ZnO thin films prepared from different pH values 8 and 11 shows good sensitivity in the range of 8.37 M $\Omega$ /%RH to 12.25 M $\Omega$ /%RH respectively. Therefore synthesized ZnO thin films can be used as a humidity gas sensor for promising potentials application.

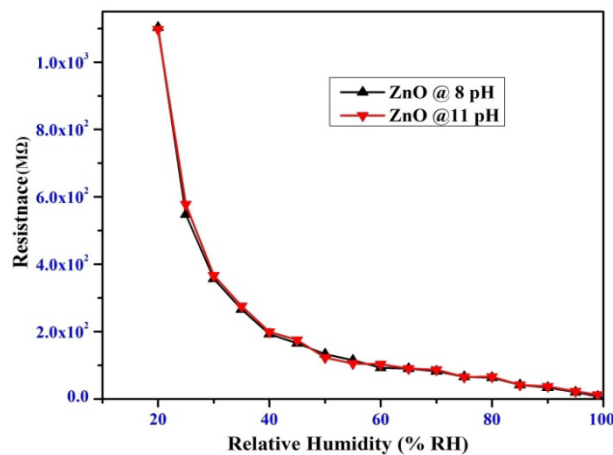


Fig. 5. Variation of resistance with change in relative humidity %RH for pH 8 and 11 of precursor solution.

### 3.5. Aging characteristic of samples

The aging effect of the nanomaterials is a very indispensable problem and significantly hindrance the application of sensing mechanism. The humidity sensing properties of ZnO thin films prepared from different pH values 8 and 11 was observed and recorded. Thereafter the aging effect of ZnO thin films were also examined using the humidity well control chamber after

6 months. The variations of resistance versus %RH of ZnO thin films revealed the aging characteristic of sample shown in figure 6 and 7. The ZnO thin films prepared at a pH values of 8 illustrate little hysteresis loop shown in variations of resistance versus %RH shown in figure 6. However ZnO thin films prepared at pH values 11 significantly less aging effect and no hysteresis loop, thus giving good quality performance up to 6 months as shown in figure 7. Thus it was observed and found that, increasing pH value from 8 to 11 leads to tuning potential application of humidity gas sensor.

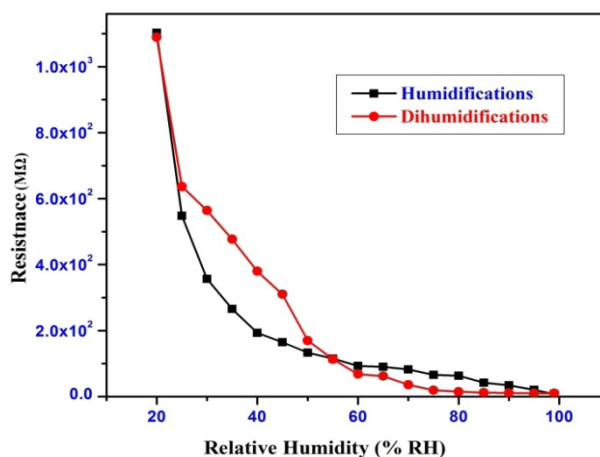


Fig. 6. Aging behavior of for pH 8 of precursor solution.

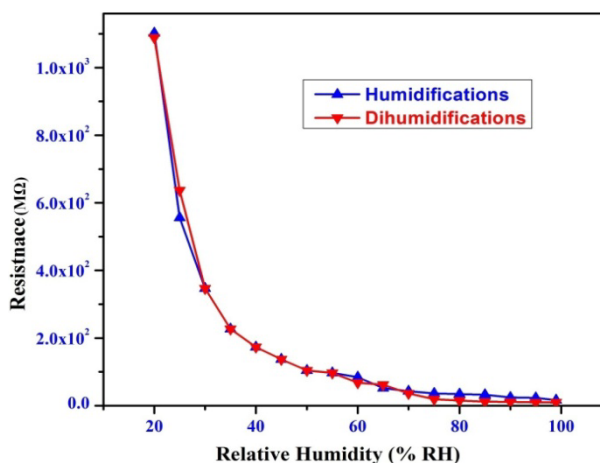


Fig. 7. Aging behaviour of for pH 11 of precursor solution.

#### 4. Conclusions

In the present work, ZnO NPs have been successfully synthesized by sol-gel method. This method is a low expensive, exceptionally simple and reproducible route for the large-scale synthesis of ZnO nanomaterials. The powder X-ray diffraction pattern exhibited prepared samples has hexagonal wurtzite crystalline structure of synthesized zinc oxide nanomaterial. The average crystalline size has been calculated from Scherer formula and found to be in the range of ~24 nm to ~30 nm. The SEM image exhibited spherical shape grains distributed throughout the surface with diameter range 80 to 95 nm. The AFM image also shows the spherical nanostructure consistently distributed throughout the surface with diameter range 75 to 80 nm. The humidity sensing properties of ZnO thin films prepared from pH values of 8 to 11 found to have good sensitivity in the range of 8.37 MΩ/%RH to 12.25 MΩ/%RH respectively.

## Acknowledgements

The authors are thankful to Research and Development plan Government of U.P. India for providing financial support. The authors are highly thankful to Department of Physics, University of Lucknow for providing the characterization facility.

## References

- [1] Geun-Hyoung Lee, *Electronic Materials Letters*, 6 (2010) 155-159; <https://doi.org/10.3365/eml.2010.12.155>
- [2] J. Yoo, J. Lee, S. Kim, K. Yoon, I. J. Park, S. K. Dhungel B. Karunagaran, D. Mangalaraj and J. Yi, *Thin Solid Films* 213 (2005) 480-481; <https://doi.org/10.1016/j.tsf.2004.11.010>
- [3] K. Keis, C. Bauer, G. Boschloo, A. Hagfeldt, K. Westermark, H. Rensmo and H. Siegbahn, *J. Photoch. Photobio. A* 148 (2002) 57-64; [https://doi.org/10.1016/S1010-6030\(02\)00039-4](https://doi.org/10.1016/S1010-6030(02)00039-4)
- [4] J Carrey, H Carr'ere, M L Kahn, B Chaudret, X Marie and M Respaud, *Semicond. Sci. Technol.* 23 (2008) 025003 (5pp); <https://doi.org/10.1088/0268-1242/23/2/025003>
- [5] A Hernandez Battez, R Gonzalez, J L Viesca, J E Fernandez, J M Diaz Fernandez, A MacHado, R Chou, J Riba, *Wear* 256 (2008) 422-428; <https://doi.org/10.1016/j.wear.2007.11.013>
- [6] Porter, F, *Zinc Handbook: Properties, Processing, and Use in Design*, CRC Press. (1991); <https://doi.org/10.1201/9781482276947>
- [7] Dapeng Wu, Zhengyu Bai, Kai Jiang, *Letters*, 63 (2009) 1057-1060; <https://doi.org/10.1016/j.matlet.2009.02.008>
- [8] H Serier, M Gaudon, M Me'ne'trier, *Solid State Sci.* 11 (2009) 1192-1197; <https://doi.org/10.1016/j.solidstatesciences.2009.03.007>
- [9] A F Lotus, Y C Kang, J I Walker, R D Ramsier, G G Chase, *Mater Sci Eng. B* 166 (2010) 61-66; <https://doi.org/10.1016/j.mseb.2009.10.001>
- [10] H Cheng, X J Xu, H HHng, J Ma, *Ceram Int.* 35 (2009) 3067-3072; <https://doi.org/10.1016/j.ceramint.2009.04.010>
- [11] A Verma, F Khan, D Kar, B C Chakravarty, S N Singh, M Husain, *Thin Solid Films* 518 (2010) 2649-2653; <https://doi.org/10.1016/j.tsf.2009.08.010>
- [12] E Hammarberg, A P Schwab, C Feldmann, *J. Colloid Interface Sci.* 334 (2009) 29-36; <https://doi.org/10.1016/j.jcis.2009.03.010>
- [13] T Ogi, D Hidayat, F Iskandar, A Purwanto, K Okuyama, *Adv. Powder Technol.* 20 (2009) 203-209; <https://doi.org/10.1016/j.appt.2008.09.002>
- [14] B D Ahn, H S Kang, J H Kim, G H Kim, H W Chang, S Y Lee, *J. Appl. Phys.* 100 (2006) 093701(1-6); <https://doi.org/10.1063/1.2364041>
- [15] R Brayner, R Ferrarilliou, N Brivos, S Djediat, M F Benedetti, F Fievet, *Nano. Lett.* 6 (2006) 866-870; <https://doi.org/10.1021/nl052326h>
- [16] P V Kamat, B Patrick, *J. Phys. Chem.* 96 (1992) 6829-6834; <https://doi.org/10.1021/j100195a055>
- [17] S Du, Y Tian, H Liu, J Liu, Y Chen, *J. Am. Ceram. Soc.* 89 (2006) 2440; <https://doi.org/10.1111/j.1551-2916.2006.01093.x>
- [18] B Ismail, M Abaab, B Rezig, *Thin Solid Films* 383 (2001) 92-94; [https://doi.org/10.1016/S0040-6090\(00\)01787-9](https://doi.org/10.1016/S0040-6090(00)01787-9)
- [19] N Lu, X Lu, X Jin, C Lu, *Polym. Int.* 56 (2007) 138; <https://doi.org/10.1002/pi.2126>
- [20] L. W. Ji, W. S. Shih, T. H. Fang, C. Z. Wu, S. M. Peng, T. H. Meen, *J. Mater Sci.* 45 (2010) 3266-3269; <https://doi.org/10.1007/s10853-010-4336-4>
- [21] X Chen, Y He, Q Zhang, L Li, D Hu, T Yin, *J. Mater Sci.* 45 (2010) 953-960; <https://doi.org/10.1007/s10853-009-4025-3>
- [22] H Zhang, D Yang, S Li, X Ma, Y Ji, J Xu, D Que, *Mater. Lett.* 59 (2005) 1696-1700;



<https://doi.org/10.1016/j.matlet.2005.01.056>

[23] W-H Zhang, W-D Zhang, J-F Zhou, J. Mater Sci. 45 (2010) 209-215; <https://doi.org/10.1007/s10853-009-3920-y>

[24] T Tsubota, M Ohtaki, K Eguchi, H Arai, J Mater Chem 7 (1997) 85; <https://doi.org/10.1039/a602506d>

[25] Ji-Y. Noh, H. Kim, Y.-S. Kim, C. H. Park, Journal of Applied Physics 113 (2013) 153703; <https://doi.org/10.1063/1.4801533>

[26] Y. Zhang, Y. Yang, J. Zhao, R. Tan, W. Wang, P. Cui, W. Song, J. Mater Sci. 46 (2011) 774-780; <https://doi.org/10.1007/s10853-010-4813-9>

[27] P Kadam, C Agashe, S Mahamuni, J. Appl. Phys. 104 (2008) 103501; <https://doi.org/10.1063/1.3020527>

[28] Y L Zhang, Y Yang, J Zhao, R Tan, P Cui, W J Song, J. Sol-Gel Sci. Technol. 51 (2009) 198-203; <https://doi.org/10.1007/s10971-009-1959-5>

[29] H X Chen, J J Ding, X G Zhao, S Y Maa, Physica B. 405 (2010) 1339-1344; <https://doi.org/10.1016/j.physb.2009.11.085>